Advanced studies on the Polycapillary Optics use at XLab Frascati

D. Hampai [a,*], S.B. Dabagov [a,b,c], G. Cappuccio [a]

[a] INFN–LNF, XLab Frascati, Via E. Fermi, 40, I-00044 Frascati (Rome), Italy
[b] RAS P.N. Lebedev Physical Institute, Moscow, Russia
[c] National Research Nuclear University MEPhI, Moscow, Russia

A B S T R A C T

X-ray analytical techniques are widely used in the world. By the way, due to the strong radiation–matter interaction, to design optical devices suitable for X-ray radiation remains still of wide interest. As a consequence of novel advanced material studies, in the last 30 years several typologies of X-ray lenses have been developed. In this work, a short review on the status of Polycapillary Optics (polyCO), from design and fabrication to various applications, has been presented making comparison of the results achieved by several groups through different X-ray optical elements.

A focus is regarded for advanced X-ray imaging and spectroscopy tools based on combination of the modern polyCO hardware and the reconstruction software, available as homemade and commercially ones. Recent results (in three main fields, *high resolution X-ray imaging*, *micro-XRF spectroscopy* and *micro-tomography*) obtained at XLab Frascati have been discussed.

1. Introduction

X-rays are used in several analytical techniques all around the world. In many cases proper optical elements for manipulating the beam are required, but having such devices for X-ray photons is not simple due to strong radiation–matter interaction. In the electromagnetic spectrum X-ray energy region is considered to be mostly comprised in the range of 1–10^2 keV.

The pioneering works of Laue [1] and Compton [2] on the reflection of X-rays by a smooth surface made possible to design an optical device capable to manage and manipulate coherent and collimated beams at grazing incidence. However, according to the Bragg condition, the relatively low interplanar distance in ordinary crystals leads to many limits on their use as X-ray optical devices. At the beginning, all powerful X-ray optics were the mirrors based on two grazing incidence schemes, one proposed in 1948 by Kirkpatrik and Baez [3], and the other in 1952 by Wolter [4]. In both cases, a very precise coincidence of the optical axis of the mirrors and a thorough treatment of the surfaces are required, and they are actually used only at synchrotron radiation facilities.

The advances in material engineering processes paved the road to extend the possibilities of configuration for grazing-incidence optics. The new optical X-ray devices can be divided in three main categories (Table 1): reflective, refractive and diffractive optics.

* Corresponding author.

In the following section a general overview on the latest status of all the optics will be done. In particular, a focus on the capillary optics state-of-the-art and the latest results achieved in different analytical fields at XLab Frascati by means of polyCO combined with conventional sources will be presented.

2. State of the art

As aforementioned, X-ray optics are divided in three main categories (Table 1), depending on the different physical operating principles. For a first approach to the different kind of X-ray optics, one can refer to [5–11].

Reflective optics are based on the total external reflection (TER) phenomenon, which occurs only if the critical incidence grazing angle θ_c is respected. This category comprises Kirkpatrick–Baez [3] and Wolter [4] mirrors. KB optics consists of two orthogonal curved mirrors and is practically employed only at synchrotron laboratories, while Wolter optics consists of two tubular rotationally symmetric TER-mirrors and is efficiently used in X-ray telescopes [12,13]. A submicron to nanometer focusing in two dimensions can be achieved.

Another class of reflective optics is represented by X-ray planar waveguides where the beam propagates in a low absorbing material enclosed between two metal layers with a lower refractive index [14]. They are one-dimensional, with the outcoming beam vertical size limited by the intermediate layer thickness down to 100 nm, and are used only at synchrotron radiation laboratories.

Table 1
X-ray optics categories scheme.

	Reflective					Diffractive	Refractive
	Kirkpatrick–Baez		Channels structures		Waveguides	Zone plates	Refractive lens
	Mirrors Kirkpatrick Baez (1948) [3]	Multilayers Underwood Barbee (1986) [20]	PolyCO Kreger et al. 1948 [21]	Capillaries Balaic et al. 1995 [22]	Feng et al. 1993 [14]	Baez 1952 [23]	Snigerev et al. 1996 [8]
E	< 20 keV	< 100 keV	< 30 keV		< 20 keV	< 30 keV	< 1 MeV
$\Delta E/E$	White beam	10^{-2}	White beam		10^{-3}	10^{-3}	10^{-3}

Fresnel zone plates (FZPs) are circular plates consisting of a series of concentric rings, working as diffraction grating for monochromatic beams by constructive interference. In the soft X-ray range FZPs can reach a resolution down to 20 nm [15], while for hard X-rays they are not very efficient [16]. Requiring very high intense and strong collimated beams, they are employed only at synchrotron radiation facilities. Nowadays, only Carl Zeiss X-ray Microscopy, Inc. couples these optics with conventional sources, obtaining a true spatial resolution down to 50 nm [17], but with a field of view between 16 and 65 μm.

Compound refractive lenses (CRL) consist of a series of cylindrical holes drilled into a single substrate [8], where the portions of matter comprised between the empty spaces forms a sort of biconcave refractive lenses. A series of these lenses is capable of focusing and collimating X-rays from 5 to 80 keV, and if combined in a crossed geometry a few microns spot can be obtained. They works very well with synchrotron radiation, but are not so efficient for conventional sources.

All these devices are characterized by a small aperture, which leads to a strong reduction in the intensity radiation. At the beginning of 80's, Kumakhov proposed a new kind of reflective optics, the capillary lenses [18,19]. The photon propagates by multiple internal total reflections along a hollow glass channel, which works as a guide also making possible to bend the X-ray beam. The critical angle is given by θ_c (mrad) = 30/energy (keV), which means very low incidence angles (1.71 mrad for 17.5 keV). These optics are formed by bundles of glass capillaries arranged in a barrel shape (full lens) in order to capture a great solid angle and focus it in a small spot, producing high flux beams, or in a half-barrel shape (semi-lenses) to convert a divergent beam into a quasi-parallel one or to collect the emitted XRF signal onto the detector. There are also straight capillaries, used for example in X-ray imaging applications to reduce the noise due to the scattering from the sample. Because of their characteristics, they can be efficiently coupled with conventional sources.

The first generation lenses were bundles of single-capillaries, then evolved in the more compact, monolithic version (second generation). In the third generation the bundles consist of polycapillaries, each one containing thousands of channels with a few microns internal diameters, and the forth generation is their monolithic version. The last generation is represented by monolithic polycapillaries micro-lenses, of smaller size and efficient also at high energies. Also monocapillary optics can be used to enhance spatial resolution and intensity in X-ray analysis; moreover the few photon reflections occurring in them do not affect the beam coherence.

Table 1 summarizes the parameters and the best achievable resolution for every class of optics.

3. PolyCO studies at XLab Frascati

For the last 15 years, at the Laboratori Nazionali di Frascati (LNF–INFN) a team of researchers has been focused on the study of X-ray optics, in particular polycapillary optical elements, being involved in several national and international projects and collaborations. This research line has resulted in the establishment of a new dedicated laboratory, XLab Frascati, which is also focused on the application of these optics for X-ray analysis in various fields, such as cultural heritage, innovative materials, medical diagnostics, pharmacology, beam diagnostics, detectors characterization, etc. The laboratory activities aim in particular to characterize novel optics and evaluate various experimental schemes for different X-ray applications such as X-ray diffraction (XRD), X-ray fluorescence (XRF and TXRF – total reflection X-ray fluorescence) and X-ray imaging. The final result of our studies is the design and development of various instrumental prototypes and new X-ray desktop facilities for advanced techniques.

Presently, two facility stations (RXR and XENA) are open to users: their combined work allows optimizing and matching the various analysis. Since 2004, XENA (X-ray Experimental station for Non-destructive Analysis) is operative. It is equipped with three X-ray Oxford Apogee tubes (W, Mo and Cu anodes), a set of mechanical components and motors for lens alignment and scanning, and an optical table providing many geometrical setup possibilities. At the beginning, being the unique experimental station, it was used for all the different X-ray analysis performed at the laboratory. Today, XENA is a facility dedicated exclusively to imaging, tomography and characterization of X-ray devices such as novel sources [24], optics [25] – diffractive crystals (Yu. Cherepennikov et al. as poster presentation at Channeling 2014) and vibrating systems (A. Liedl et al. as poster presentation at Channeling 2014) – and detectors (A. Gogolev et al. as oral presentation at Channeling 2014).

RXR (Rainbow X-ray) is an optimized system of previous versions [26,27] for 2D/3D XRF micro-imaging and TXRF. It is equipped with two detectors of different energy efficiency, in order to measure a full spectrum ranging from 800 eV to 25 keV. RXR works in confocal mode: the source is coupled with a full-lens, and both the detectors are combined with dedicated half-lenses. RXR is also equipped with an optional vacuum chamber for measurements in the low energies range. This vacuum chamber has the possibility of inserting a polyCO for TXRF analysis.

The main characteristics of XLab Frascati are summarized in Table 2. An homemade software (Vitruvio) for the simultaneous control of both the stations has been developed. This system is divided in three main sections: the "user" level, the spooler and the hardware components. Such an arrangement allows a total control of the stations with a simple code. The software, written in LabView, is based on the state machine model.

3.1. μXRF spectrometry and imaging

In the XENA cabinet, μXRF punctual measurements are carried out by combining one of the three X-ray tubes with a polyCO full-lens having an Input Focal Distance (IFD) of 56.5 mm, an Output Focal Distance (OFD) of 44 mm, a length of 12 cm, and a

Table 2
XLab Frascati facilities.

	XENA	RXR
Station	**X**-ray **E**lemental station for **N**on-destructive **A**nalysis	**R**ainbow **X**-**R**ay
Analysis	(1) High resolution imaging (2) μCT (3) X-ray optics characterization (4) Detector characterization (5) Novel sources	(1) μXRF (2D and 3D mapping) (2) TXRF
Resolution	(1) < 1 μm (with LiF detector)	(1) <50 × 50 μm^2 <50 × 50 × 50 μm^3 (step resolution combined with the polyCO)
	(2) <17 × 17 × 17 μm^3 (CT with spatial resolution CCD camera of 10.4 × 10.4 μm^2)	(2) ppb concentrations
		(3) <135 eV at 5.9 keV (with the SDD detector)

focal spot size of 100 μm. The tubes work at a maximum voltage of 50 kV and current of 1 mA. The same energy dispersive Silicon Drift Detectors (SDD) employed in RXR can be used for it. By this way, the elemental composition of inorganic samples can be obtained. With the same devices, but different geometrical setup, polycapillary lenses can be also characterized, ([28] and C. Polese et al. as poster presentation at Channeling 2014).

The same setup combined with motorized sample stages is used for 2D elemental mapping. The motors have a step of 1 μm. Different 2D μXRF imaging have been carried out on cultural heritage samples (painting cross section, *adobe* [29]). In Fig. 1, a 2D XRF scan on a sample of cultural interest, a glazed pottery, is shown. The tube was set at 35 kV and 750 μA, and the acquisition time was 20 s for each spectrum, with a step scan of 25 μm. The elemental distributions obtained for potassium, sulfur, iron and lead are illustrated. The good separation between K, S and Fe areas, combined with the axis movement parameters, allows the internal resolution of the system to be estimated.

3.2. Total reflection X-ray fluorescence (TXRF)

Changing the geometry setup, and by means of a CCD camera for the system alignment, total reflection XRF analysis for low

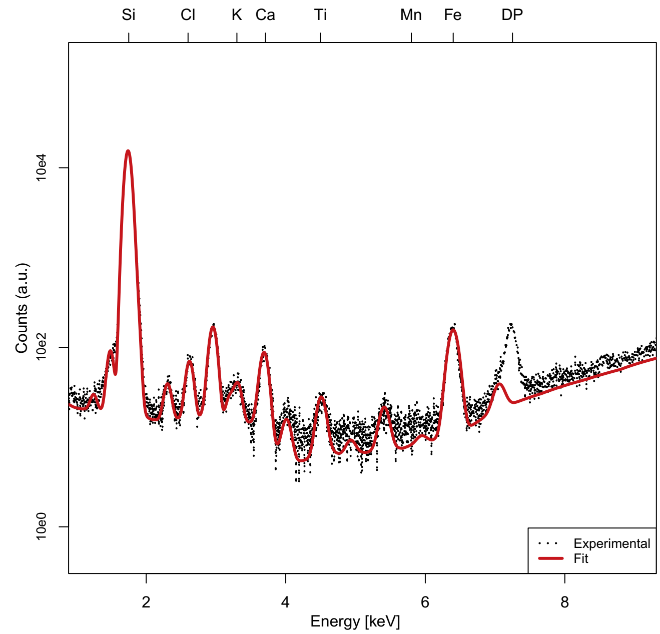

Fig. 2. TXRF spectrum of insoluble dust from an Antarctic ice core.

concentration samples can be performed. Preliminary studies have allowed detection limits under 10 ng for 10 elements (Si, Cl, Ar, K, Ca, Ti, Cr, Mn, and Fe) to be achieved (Fig. 2) [27].

3.3. X-ray imaging

XENA is equipped also for X-ray micro-radiography and micro-tomography, with two CCD camera from Photonic Science, with a spatial resolution of 3.5 × 3.5 μm^2 and 10.4 × 10.4 μm^2 respectively. A motorized stage is used for the sample rotation. Many imaging studies have been carried out on different materials, such as biological samples (ant, bud), cultural heritage samples, geological samples, high pressure fuel sprays ([30–32] and L. Marchitto et al. as oral presentation at Channeling 2014).

In Fig. 3 a high resolution tomographic reconstruction obtained with XENA for a synthetic emerald [33] is shown. The experimental parameters (720 images for 360°, 120 ms/image, Cu anode,

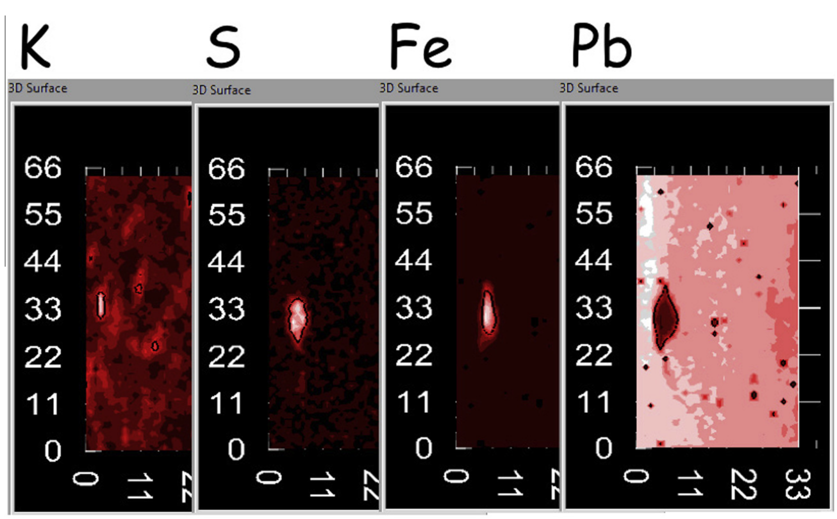

Fig. 1. 2D μXRF scan of a glazed earthenware sample. Elemental maps of K, S, Fe and Pb are shown. The spatial resolution (<50 μm) allowed the K, S and Fe areas to be identified, although the singular contributions are very close.

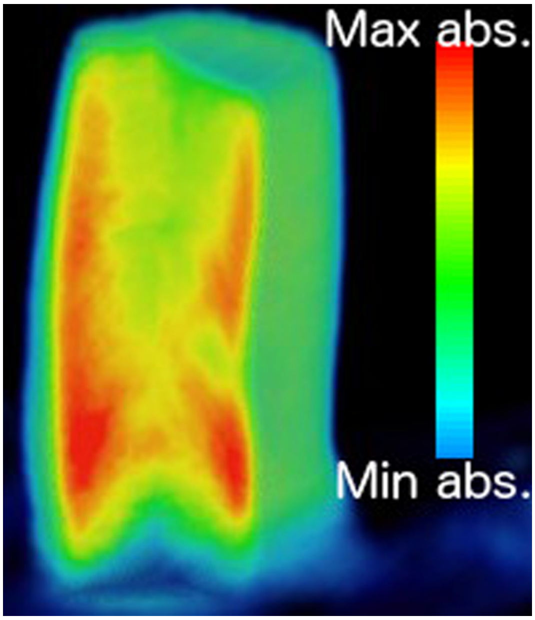

Fig. 3. Tomographic image of a synthetic emerald: the red zone indicates the higher absorbance area, revealing the chromium distribution in the crystal. (For interpretation of the references to colour in this figure legend, the reader is referred to the web version of this article.)

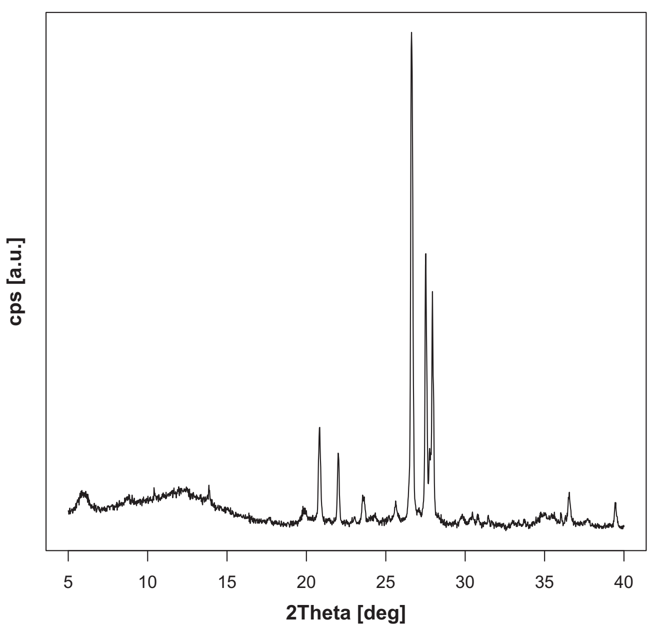

Fig. 4. XRD spectrum of an *adobe* sample. Quartz, plagioclase and feldspar are the major constituents, but also weak amounts of phyllosilicates close to chlorite and illite were detected by the reflections at around 6.0° and 8.70° 2θ. The plagioclase phase was found to match closely the JCPDS card 09–0466 of albite, $NaAlSi_3O_8$.

35 kV/700 μA for a total radiation exposition of 600 s) allows a ∼16 μm resolution to be obtained.

High resolution X-ray imaging analysis based on the combination of polycapillary lenses with GEM, in the framework of the Gemini project, and LiF detectors [34,35] within the iFCX project, achieving submicron spatial resolution, have been carried out.

3.4. X-ray diffraction (XRD)

The XLab Frascati laboratory is equipped also with a Seifert X-ray diffractometer θ–2θ. Its Cu anode X-ray tube has the possibility to be coupled with a half-lens to obtain a parallel beam for thin film analysis or a full-lens for micro-diffraction. By this way, also the mineralogical composition of the samples can be obtained, in order to integrate the informations achievable with the other techniques available at the facility (Fig. 4).

4. Conclusions

In this work we have presented a review and comparison on the status of X-ray optics, with a particular attention to the Polycapillary Optics. It has been shown that the results achieved at XLab Frascati by PolyCO combined with conventional X-ray sources are comparable with those obtained by means of other optics coupled with synchrotron radiation sources.

XLab Frascati has two independent user-facilities (XENA and RXR) dedicated to imaging, tomography and fluorescence (μXRF e TXRF) analysis. The latest results obtained for each experimental station have been presented.

References

[1] W. Fridrich, P. Knipping, M. von Laue, Sitzungsber. Bayer. Akad. Wiss. 303 (1912).
[2] A.H. Compton, Philos. Mag. 45 (1923) 1121.
[3] P. Kirkpatrik, A.V. Baez, J. Opt. Soc. Am. 38 (1948) 766.
[4] H. Wolter, Ann. Phys. (Leipzig) 10 (1952) 286.
[5] H. Mimura, H. Yumoto, S. Matsuyama, et al., Appl. Phys. Lett. 90 (2007) 051903.
[6] O. Hignette, P. Cloetens, C. Moraweey, et al., AIP Conf. Proc. 879 (2007) 792799.
[7] D.H. Bilderback, S.A. Hoffman, D.J. Thiel, Science 263 (1994) 201–203.
[8] A. Snigirev, V. Kohn, I. Snigireva, et al., Nature 384 (1996) 49.
[9] A. Jarre, C. Fuhse, C. Ollinger, et al., Phys. Rev. Lett. 94 (2005) 074801.
[10] H.C. Kang, J. Maser, G.B. Stephenson, C. Liu, et al., Phys. Rev. Lett. 96 (2006) 127401.
[11] C.G. Schroer, O. Kurapova, J. Patommel, et al., Appl. Phys. Lett. 87 (2005) 124103.
[12] chandra.harvard.edu.
[13] xmm.esac.esa.int.
[14] Y.P. Feng, S.K. Sinha, H.W. Deckman, et al., Phys. Rev. Lett. 71 (1993) 537–540.
[15] W. Chao, B.D. Harteneck, J.A. Liddle, et al., Nature 435 (2005) 1210–1213.
[16] B. Nöhammer, C. David, M. Burghammer, C. Riekel, Appl. Phys. Lett. 86 (2005) 163104.
[17] www.zeiss.com.
[18] M.A. Kumakhov, F.F. Komarov, Phys. Rep. 191 (5) (1990) 289–350.
[19] S.B. Dabagov, Phys. Usp. 46 (10) (2003) 1053–1075.
[20] J.H. Underwood, T.W. Barbee, C. Frieber, Appl. Opt. 25 (1986) 1730–1732.
[21] D.R. Kreger, Rec. trav. bot. nérlandais 41 (1948) 603.
[22] D. Balaic, K.A. Nugent, Appl. Opt. 34 (1995) 7263–7272.
[23] A.V. Baez, J. Opt. Soc. Am. 51 (1961) 405–412.
[24] Nanoray, a portable X-ray machine, FP7 Project N 222426 (2008–2011).
[25] D. Hampai et al., Spectrochim. Acta B 64 (11) (2009) 1180–1184.
[26] D. Hampai, S.B. Dabagov, G. Cappuccio, et al., Opt. Lett. 33 (23) (2008) 2743–2745.
[27] D. Hampai, S.B. Dabagov, C. Polese, et al., Spectrochim. Acta B 101 (2014) 114–117.
[28] C. Polese, S.B. Dabagov, A. Esposito, et al., AIP Adv. 4 (2014) 077128.
[29] A. Liedl, Master thesis.
[30] L. Allocca, L. Marchitto, S. Alfuso, et al., AIP Conf. Proc. 1221 (2010) 191.
[31] L. Allocca, S. Alfuso, L. Marchitto, et al., ICLASS Proc. (2012).
[32] D. Hampai, L. Marchitto, S.B. Dabagov, et al., Nucl. Instr. Meth. B 309 (2013) 264–267.
[33] F. Bellatreccia, G. Della Ventura, M. Piccinini, O. Grubessi, N. Jb. Miner. Abh. 185 (1) (2008) 11–16.
[34] D. Hampai, S.B. Dabagov, G. Della Ventura, et al., Europhys. Lett. 96 (6) (2011) 60010.
[35] D. Hampai, F. Bonfigli, S.B. Dabagov, et al., Nucl. Instr. Meth. A 720 (2013) 113–115.